WATER RESOURCES RESEARCH, VOL. 39, NO. 6, 1148, doi:10.1029/2002WR001437, 2003

Development and evolution of rill networks under simulated rainfall

J. A. Gómez
Instituto de Agricultura Sostenible, Consejo Superior de Investigaciones Científicas, Cordoba, Spain

F. Darboux
Laboratoire de science du sol, Institut National de la Recherche Agronomique, Olivet, France

M. A. Nearing
Agricultural Research Service, USDA, Tucson, Arizona, USA

Received 8 May 2002; revised 12 December 2002; accepted 3 March 2003; published 10 June 2003.

[1] The evolution of drainage networks at large scales has been shown to follow a principle of minimization of the global rate of energy dissipation. This study was undertaken to evaluate whether a principle similar to that holds for rill networks at a much smaller scale. Simulated rainfall was applied to a 2 m by 4 m flume with varied initial slope (5% and 20%) and roughness (low, moderate, and great) conditions. The results indicated that assuming the validity of a local optimality principle, the rill networks evolved according to a global principal of energy optimization in situations where rilling was intense, 20% slope, but not at 5% slope where diffusive processes played a dominant role in the overall erosion process. These results suggest that the application of models similar to some used to explain the evolution of river networks may have a role in understanding the initiation and evolution of rill networks in situations of intensive rilling. Our results and analysis suggest that further experiments might be undertaken to study the spatial distribution of flow velocity within the rill networks at a given flow discharge and the local rate of energy dissipation at rill links. Despite the convergence toward similar values of some of the network characteristics, differences in the microrelief of the initial surfaces were translated into significant differences between the final rill networks. *INDEX TERMS:* 1848 Hydrology: Networks; 1878 Hydrology: Water/energy interactions; 1815 Hydrology: Erosion and sedimentation; 1824 Hydrology: Geomorphology (1625); *KEYWORDS:* rill networks, energy dissipation, microrelief, evolution, drainage networks

Citation: Gómez, J. A., F. Darboux, and M. A. Nearing, Development and evolution of rill networks under simulated rainfall, *Water Resour. Res.*, *39*(6), 1148, doi:10.1029/2002WR001437, 2003.

1. Introduction

[2] The regularity of river systems and the similarity often exhibited by river drainage networks have attracted the attention of geomorphologists for a long time, e.g., Playfair in the work of *Tarr and Martin* [1914]. The similarity between rill networks developed on eroding slopes and river drainage networks has also been noted and studied for a long time. This similarity is not surprising since rills belong to the same drainage network that river sections do [*Leopold et al.*, 1964]. Nevertheless many studies distinguish between rill and river scales because there are significant differences between them due to their different sizes and the more discontinuous and ephemeral character of the rills compared to rivers [*Knighton*, 1998]. This difference in size implies that some mechanisms involved in the evolution of rill networks may seldom be present in the evolution of river networks. For that reason the interpretation of rill network processes from the experimental and theoretical studies of river networks may not be straightforward, in the same way that the interpretation of the evolution of river networks from small-scale rill studies has its shortcomings [*Knighton*, 1998].

[3] Several laboratory studies have documented similarity between river and rill networks [*Mosley*, 1974; *Parker*, 1977; *Ogunlela et al.*, 1989; *Wilson and Storm*, 1993]. Other laboratory studies have shown similarity between drainage networks at basin and small scales, although the similarity between rill and river networks is not completely understood [*Helming et al.*, 1998].

[4] One of the reasons behind the search of the degree of similitude between rills and river networks is that if such a relationship exists, researchers working at the hillslope scale may use knowledge developed at the river scale to understand and model rill network processes. Rill processes are critical components of process-based runoff erosion models, like WEPP [*Flanagan and Nearing*, 1995] and EUROSEM [*Morgan et al.*, 1998], although the development of the rill networks at hillslope and plots of the scale of tens of meters (where most of the data used to develop those models come from) remains relatively poorly understood, as shown by the

0043-1397/03/2002WR001437$09.00

active research in this area [*Helming et al.*, 1998; *Favis-Mortlock et al.*, 2000]. A better understanding, description, and modeling of rill network evolution would increase our comprehension of erosion processes at the hillslope scale, and might increase the prediction capabilities of future erosion models.

[5] The study of river networks has evolved from descriptive [*Horton*, 1945] and random topological analysis [*Shreve*, 1966] toward physical theories. We do not intend to make a review of those theories here, but rather only to introduce some of those most relevant to our study. A thorough review of these theories is given by *Rodríguez-Iturbe and Rinaldo* [1997]. Theories of minimum stream power and energy dissipation have been used to describe channels in equilibrium with water and sediment based on analogy with thermodynamic systems [*Yang*, 1971a, 1971b; *Song and Yang*, 1980; *Yang et al.*, 1981] and in the context of geomorphic research [*Howard*, 1971, 1990; *Roy*, 1985]. *Rodríguez-Iturbe et al.* [1992] proposed a theory of the evolution of river networks according to two hypothesis of optimality in energy expenditure. The first is a local optimality principle that states that river networks adjust their channel properties toward a state in which the energy expenditure per unit area of channel is the same everywhere in the network. The second hypothesis is a global optimality principle that states that river networks adjust their topological structure toward a state in which the energy expenditure of the whole network is minimum. The first hypothesis implies that the average flow velocity within the network tends to be constant; something supported by field observations, although this may not be a universal behavior.

[6] The mathematical formulation of the total energy expenditure of the network according to *Rodríguez-Iturbe et al.* [1992] is:

$$E = \sum_{i=1}^{i=n} P_i = k \sum_{i=1}^{i=n} Q_i^{0.5} L_i \qquad (1)$$

where i is the link number, n is the total number of link networks, E and P_i are the rates of energy expenditure for the network and an individual link respectively, both having units of power [$M\ L^2\ T^{-2}$], Q_i [$L^3\ T^{-1}$] is the link flow discharge, L_i [L] is the link length, and k is a constant for all the links throughout the network for a given flow condition. They derived from their theory hydraulic relationships, $w = (\text{const.})\ Q^{0.5}$, and $d = (\text{const.})\ Q^{0.5}$, with w meaning width and d depth, that approximate those obtained from field observations in rivers at bank-full conditions. Using this theory, *Rodríguez-Iturbe et al.* [1992] simulated channel networks by minimization of E in a virtual basin that showed topological properties similar to those of actual river networks. A detailed discussion of optimal channel networks in basins with simple and multiple outlets is given by *Rodríguez-Iturbe and Rinaldo* [1997].

[7] Recently, *Banavar et al.* [2001] have shown that the global minimum is not a hypothesis, but an exact property of the stationary state of the general landscape evolution, although some of the assumptions made in their study imply that these findings do not need to apply necessarily at hillslope scales. For example, their analysis of drainage basins assumes certain degree of smoothness that holds at long length scales, from tens to a few hundred meters, well above of the characteristic scales of hillslope processes.

[8] The objectives in our laboratory study of rill networks were two-fold. The first was to develop a dataset of the evolution of rill networks and their properties through successive simulated rainstorms under different slopes and roughness. The second objective was to study the evolution of the rill networks on small hillslopes according to the principle of global minimum rate of energy expenditure as proposed by *Rodríguez-Iturbe et al.* [1992].

2. Material and Methods

[9] We performed our experiments in a flume 2-m wide and 4-m long. The six experimental treatments consisted of two different slope steepnesses (20 and 5%) at three different initial surface conditions: low roughness (hereafter LR); medium oriented roughness (hereafter MR); and large un-oriented roughness (hereafter GR).

2.1. Flume and Soil Preparation

[10] The flume was built with free drainage at the bottom. It consisted of a rectangular box, open at the top and the bottom, surrounding a small, sloped soil bed. This slope was formed by a 0.05-m deep gravel layer, on top of which a sand slope was prepared. The depth of the sand slope varied according to the slope steepness. The minimum sand depth was 0.05-m at the flume outlet. The maximum sand depth, at the highest point of the surface, was 0.85-m and 0.15-m for the 20% and 5% slope, respectively. A layer of topsoil, 0.28-m thick, was placed on top of the sand.

[11] The soil used was a Camden Soil (Fine-silty, mixed Typic Hapludalf) collected from the Tippecanoe County, Indiana. The natural consolidated soil has a bulk density between 1.3–1.5 g/cm^3, and an organic matter content between 1 and 2 % [*Ziegler and Wolf*, 1998]. All the soil was air dried and sieved through a 2-mm screen to insure homogeneity. The soil was placed in successive layers of 0.06-m thickness, except the final top layer of 0.04-m. The procedure to place each soil layer was as follows: First the receiving surface was slightly raked and the soil was spread. After homogenously distributing the soil with hands and rakes, it was slightly packed using a 5 kg weight. The surface was covered with a geotextile material (to prevent surface sealing) and 30 mm of rainfall were applied for approximately three hours. The geotextile material was removed, and the cracks and depressions observed on the surface 72 hours after the rain were filled with more dry soil and the surface reshaped. We waited 5 days after reshaping the surface before placing a new soil layer, and the same steps were repeated until reaching the level of the flume outlet that remained at a constant level throughout the whole experiment. That situation, i.e., no base level change, is that which exists in most of the runoff plots used in previous rill and erosion experiments, although experiments with variable base level have been reported [e.g., *Parker*, 1977]. We changed the slope steepness by modifying the profile of the sand base. With this design the networks in our analysis were not in dynamic equilibrium as is usually assumed in many studies of basin evolution, but were an approximation of that ideal state. Dynamic equilibrium means that the erosional loss and the tectonic uplift are approximately in balance everywhere in the basin. Our networks exhibited

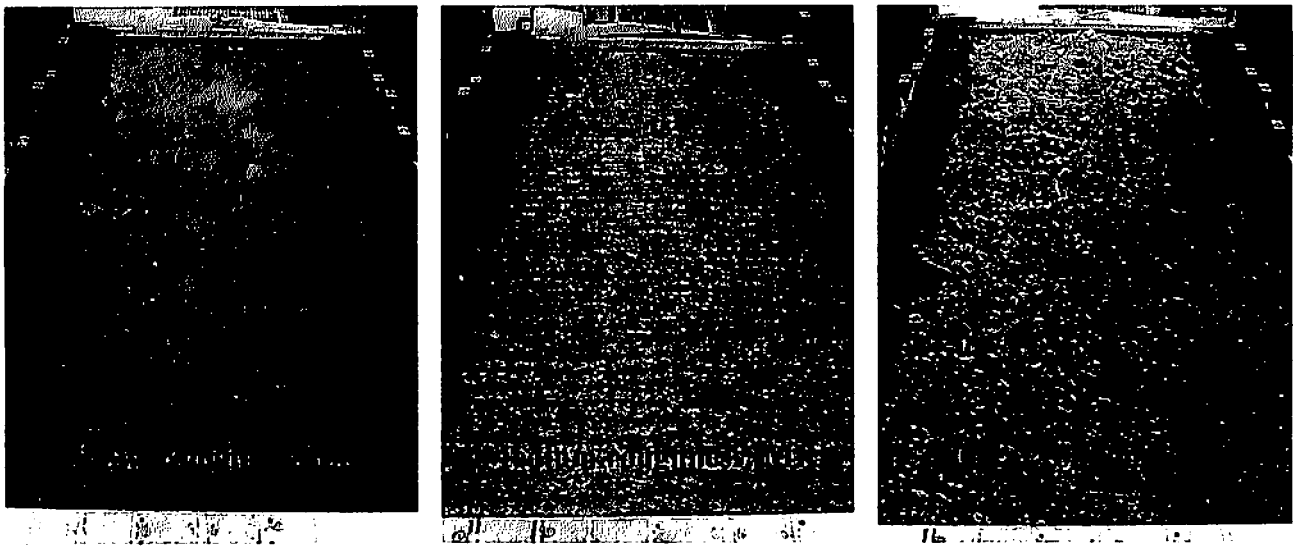

Figure 1. Initial surfaces.

only a small decrease in the average flume surface level compared to the total elevation difference within the flume.

[12] The low roughness surface, LR, was the first surface to be prepared for each set of experimental replications. The procedure described in the previous paragraph ensured a very smooth surface. The other two surfaces, medium roughness, MR, and great roughness, GR, were prepared by simulating tillage on the surface using two different tools. A hand hoe (the blade 0.15-m wide and 0.1-m long) was used for the GR, creating a very rough, nonoriented surface. A garden weasel used perpendicularly to the direction of the maximum slope was used for MR, creating a surface with an oriented roughness, intermediate between GR and LR. We chose those treatments in order to create very different surface situations (understood as causing a simultaneous modification of surface roughness and bulk density) that were easy to replicate, but which did not create a situation where the combination of large oriented roughness and a relatively narrow flume would concentrate the runoff toward the flume walls. Figure 1 shows the initial surfaces.

[13] The following procedure was adopted to perform tillage under similar conditions of soil moisture and density. After the experiment on the LR surface was finished, we let the soil dry for 7 days. Then, we added additional dry soil to the flume until reaching the original soil level to compensate for sediment losses. The top 0.15-m of the soil was turned over and thoroughly mixed. The surface was carefully leveled until obtaining a smooth surface. At this point we applied a 2-hour of rainfall at 15-mm/h in successive steps (stopping and waiting several hours when surface runoff became significant) until completing 2-hours of rainfall time on the bare surface. The soil surface was then allowed to dry for 8 days using fans, and finally a manual tillage was performed two days before starting the experiment. When the experiment on this surface was finished, we repeated the whole procedure to prepare the third remaining surface condition, MR or GR. When the first replication of the three treatments (LR, MR and GR) was completed, the top 0.16-m of the soil was replaced by new soil and the simulations corresponding to the second replication were started. In this second replication we changed the order between GR and MR compared to the first replication, but we always started with the LR surface.

[14] Table 1 gives a description of the surface bulk densities (0.05-m topsoil layer), measured using the excavation method [*Blake and Hartge*, 1986], of the initial and final surfaces. It also shows the roughness of the initial surfaces using two different indexes: the standard deviation of the individual elevation readings after removing the effects of slope and (for the case of MR, only) oriented roughness, RC index [*Currence and Lovely*, 1970]. The second index used, the tortuosity index, T [*Boiffin*, 1984], is the ratio between actual and projected (on the horizontal plane) length of a profile of the soil surface calculated after slope and oriented roughness effects were removed. In our case the profiles were made in the direction perpendicular to the main slope. The spacing between two consecutive profiles was 0.0015 m, totaling 2368 profiles per analyzed flume surface. The elevation readings for the roughness determination come from a digital elevation model, DEM, at 1.5-mm grid spacing of each of the three original surfaces.

2.2. Rainfall Simulations

[15] Each experiment consisted of 5 consecutive rainfall simulations for each replication of a treatment starting on a freshly prepared surface. The rainfall simulations lasted 1-h each and were timed 48-h apart. Our objective was to apply rainfall intensities that induced the formation of rill networks on the flume surface at a rate such that differences in network development between consecutive rainfalls could be observed. To allow a better interpretation of our

Table 1. Characteristics of the Initial and Final Surfaces[a]

Treatment	bd, Kg m^{-3}	RC, mm	T
GR	940	26.24	1.75
MR	1020	8.23	1.63
LR	1140	2.55	1.02
Final surface	1250		
Subsurface layers	1220		

[a]Here bd is bulk density, RC is roughness, and T is tortuosity.

results, the rainfall intensities were the same for both slope steepnesses. In order to achieve such objectives, the first three rainfalls had an intensity of 45 mm h^{-1}, and the last two 60 mm h^{-1}. With the three first rainfall simulations we observed in the same experiment the evolution of the network under constant rainfall intensity, which resulted in approximately similar runoff rates. The last two rainfall simulations at 60 mm h^{-1} were introduced for the case of rill development at the 5% slope, for which the rainfall intensity of 45 mm h^{-1} was not great enough to cause sufficient rill development. With this experimental design the networks operated under bank-full discharges for each treatment. This is the situation that is likely to yield the same type of results, regarding the principles of optimal energy expenditure, as the mean annual (maintaining) discharge [*Rodríguez-Iturbe and Rinaldo*, 1997]. Agronomists use 48-hours as a rule of thumb to estimate the period when most of the gravitational movement of the water infiltrated after a rainfall event takes place. Although crude, we chose that interval in order to start the simulations with approximately similar soil water content, while at the same time minimizing the duration of the experiment. The initial soil water content was measured using 10 TDR probes, 0.15-m length, inserted vertically in the areas of the flume surface near its perimeter. We depended on control of the rainfall and drying time during the surface preparation to minimize the differences in soil moisture content at the beginning of the first rainfall simulation. The average volumetric water content at that time for the 12 experiments was 20.7% (standard deviation 1.1%) without significant differences between different treatments.

[16] Rainfall intensity was monitored during each rainfall simulation using 8 rain gages located on the flume edges. The monitoring of intensity showed that the rainfall intensities remain stable throughout the duration of the experiment, with a coefficient of variation of 2.4%.

[17] During each rainfall simulation runoff samples were taken at the flume outlet at two minutes intervals from the moment that runoff started. These samples were used to calculate the runoff and sediment fluxes. After the first rainfall simulation, seven drainage links (defined as sections between consecutive junctions) were selected on the flume surface. For this selection of drainage links, we defined drainage areas as areas of rill incision or, in their absence, areas where we observed flow accumulation during the previous rainfall using dye tracer. The criterion was to include two samples within each of these length ranges: 0.25–0.5 -m, 0.5–1.0 -m, and larger than 1.0-m. In these links, mean flow velocity was measured using the leading edge fluorescent dye technique with the correction coefficient proposed by *King and Norton* [1992]. Measurements were taken in each of these seven rills during each of the last four rainfall simulations at two times (approximately minutes 25 and 45) with two replications each. When necessary, we delayed the timing of the first reading until the runoff rate measured at the end of the flume reached an approximately steady value. Flow velocity for each simulation was computed as the average of the four measurements taken at each link. After the final rainfall simulation, mean flow velocity at known flow discharge (without application of rainfall) was measured in each of the seven rills, and the relationship between sediment flux at different flow discharge was measured in one of the seven rill links selected.

2.3. Digital Elevation Models

[18] The whole flume surface was measured using a laser scanner at six different times for each treatment and replication. The first scan was performed on the original undisturbed surface and the other five were taken after each rainfall. From these six scans we derived six digital DEMs of the flume surface. The laser scanner used was described in detail by *Darboux and Huang* [2003]. The scanner was able to measure the micro-topography of a 0.5-m by 4-m surface with a resolution of 0.5-mm in the Z (elevation), and X directions, and 1.5-mm in the Y direction. Six scan strips were needed to measure the whole surface of the flume. They were combined to obtain a DEM at a 1.5-mm regular grid. The cells where elevation readings were missing due to the blocking of the line of view of the scanner camera by surface features were interpolated as the average of the elevation of the surrounding cells.

[19] We did not use all the area covered by the DEMs in our analysis. We selected a rectangular area 1.8-m wide by 3.6-m long. We left out of the analysis the 0.1-m wide strips close to the flume's longest sides and the final 0.4-m wide strip closest to the flume outlet. There were three reasons for this decision. The first was that in these areas the vision to the laser camera was obstructed by metal pieces used as reference points in a close range photogrammetry experiment performed on the flume at the same time. The second reason was that the length of the scanner (4-m) was not sufficient to cover the whole length of the flume in a single sweep, because the scanner had to be used parallel to the flume surface, which was longer than 4-m due to inclination. Thirdly, removal of the last 0.4 m of the bed eliminated end effects caused by the outlet of the flume, which are typically difficult to interpret in laboratory erosion experiments. We resampled the DEMs from the 1.5-mm to obtain a 3-mm grid size, and all the drainage network analyses were made using the 3-mm grid. We chose the larger grid size to reduce the size of the files used, which greatly facilitated their manipulation and storage. Consistency with future simulations studies was also a consideration in this decision. The size of the original 1.5-mm grid size files becomes a limiting factor due to the large computational time required if we intend to use these DEMs as inputs to some of the models of rill initiation currently available, e.g., Rill-Grow (Favis-Mortlock personal communication).

[20] *Gyasi-Agyei et al.* [1995] suggested that a DEM is adequate for extracting the drainage network if the ratio of average pixel drop and vertical resolution is greater than unity, i.e.,

$$\frac{\text{average pixel drop}}{\text{vertical resolution}} \approx \frac{\alpha D_X}{\sigma_{\Delta Z}} \tag{2}$$

where α is the mean slope (m/m), D_x is the grid point spacing (3-mm in our DEMs) and $\sigma_{\Delta Z}$ is the standard deviation of the relative error in elevation that was calculated according to equation 3 [*Walker and Willgoose*, 1999].

$$\sigma_{\Delta Z} = \sigma_Z \sqrt{1 - \rho_1^2} \tag{3}$$

where σ_z is the standard deviation of absolute error in elevation, and ρ_1 is the lag 1 correlation of the absolute error in elevation. We did not have independent values of the coordinates of the points scanned, so we estimated the absolute error using the coordinates of the points corresponding to two aluminum beams located on the extremes of the flume, which appear in all the DEMs. The absolute difference in elevation was estimated as the difference between the readings in elevation and the regression line calculated using the X and Z coordinates of the same points. We used the differences with the regression line, which represents the (assumed) perfectly straight beam, as a surrogate index of the absolute error. A sub sample of DEMs for the experiments at 5 and 20% slope steepness were analyzed, and all of them showed a ratio for equation 2 greater than one. This is only a necessary condition [*Gyasi-Agyei et al.*, 1995], but it suggests that the quality of the DEMs was appropriate for our analysis. Additionally, some of the DEMs were compared to DEM's of the same surface obtained by close range photogrammetry. While this second technique showed a better relative accuracy, no artifacts or significant deviations were detected in the laser-generated DEM's during this comparison [*Rieke-Zapp et al.*, 2001].

2.4. Drainage Network Delineation and Analysis

[21] The analysis of the drainage network evolution was based on the properties of the drainage networks delineated from the DEMs. Several steps were required for this. The first was the processing of the surface to eliminate sinks and closed depressions. For this task we used Topaz ver. 3.12 [*Garbrecht and Martz*, 1997]. The second step was the calculation of the contributing area for each cell. We accomplished this using the steepest descent algorithm, commonly known as D8, [*O'Callaghan and Mark*, 1984]. Finally, the recognition of the drainage network was made considering those cells having a contributing area higher than a critical threshold area, CSA, to be part of the network. This method is used in most of the studies of drainage networks from DEMs. The CSA was determined empirically as follows. After each one of the 5th rainfall simulations we made a survey of the flume surface, counting the number of rills and measuring their depth and width at 5 transects. We defined a rill in our survey of the flume surface as an area where both flow convergence was observed during the rainfall simulation and incision of the soil surface could be visually identified after the rainfall simulation. To aid in recognizing these areas of flow concentration, pictures were taken of the flume surface at different times during the rainfall simulations after application of dye tracer. These five transects were located at 0.4, 1.26, 2.2, 2.8 and 3.5-m from the upper end of the flume. Simultaneously we delineated the drainage network for the DEM corresponding to the same flume surface where we made the transects, using the method previously describe and an arbitrary CSA value. On that delineated drainage network, we made five virtual transects counting the number of network links at 0.4, 1.26, 2.2, 2.8 and 3.5-m from the upper end of the flume. Repeating this process, making virtual transects for networks delineated using different CSA values, we calculated by trial and error the CSA value that gave a total number of network link counted in the virtual transects (sum of the link counted at the five transects) equal to the total number of rills counted in the transects on the flume surface. In this way a CSA value was calculated for each treatment and replication. The CSA value was used in the definition of the drainage network for the six surfaces corresponding to that experiment. Using this procedure we assumed CSA to be constant in space and time. The experiment was designed in an attempt to provide the maximum possible spatial homogeneity in soil surface properties and rainfall intensity for a given treatment. This homogeneity supports the use of a constant CSA in space, since the complex interactions between climate, soil, vegetation, etc., present in natural networks and justifying spatially varied CSA are not present. We used also a CSA constant in time (from the 1st to the 5th rainfall simulation). This decision was taken to keep our analysis comparable to previous studies of drainage networks, in most of which the same support area has been used through time [e.g., *Rinaldo et al.*, 1992; *Helming et al.*, 1998]. We note that according to our definition, the CSA increases noticeably with drainage density, which is expected to increase with cumulative rainfall as well as with rainfall intensity. A consequence of our definition of CSA is that in this study we analyzed the evolution of drainage networks that corresponded to the rill network after the fifth rainfall or to areas of flow concentration carrying a similar amount of runoff in previous stages. We assumed that these areas were the precursors of the rills. To have an account of how much this CSA varied with successive rainfall simulations for the same treatment, although we have chosen to use a constant one, the same procedure was followed after each rainfall simulation, and a CSA value was calculated for each treatment and rainfall simulation, except for the original surface whose CSA was considered to be that corresponding to the surface after the first rainfall simulation.

[22] Finally, we compared the delineated network using the D8 algorithm with the multiple flow direction algorithm of *Quinn et al.* [1991] using the same CSA value. We did this to visually evaluate if the method of calculating the contributing area had an important effect in the delineated network for the conditions and scale of our study.

[23] Network link was defined according to the Horton-Strahler approach [*Knighton*, 1998]. Link length, L_i, was calculated as the sum of the flow lengths through all the grids (as defined by the 3 mm grid spacing discussed above) intersected by that particular link. The flow length through grids with a straight lateral or longitudinal flow direction was equal to the grid length, and flow length through grids with diagonal flow direction was equal to the hypotenuse of the grid length. Link slope, S_i, was calculated as the difference in elevation between the initial and final point divided by the link length. Link orientation, O_i, was defined by the absolute value of the angle formed by the intersection of the line that goes trough the initial and final points of the link with a line parallel to the flume's longest side (downslope direction) that passed through the lowest point of the link. In this definition, 0° means that the link flows parallel to the flume's longest side (or in other words, the direction of the main slope in the flume). Link contributing area, A_i, was defined as the number of cells that drain via surface runoff through the final cell of the link. Drainage density was defined according to *Horton* [1945]. The energy expenditure of the water flowing through the each link

Table 2. Average Final Runoff Rates for the Different Treatments and Rainfall Simulations

Slope	Treatment	Rainfall Event 1	2	3	4	5
20%	GR	40	42.6	42	58.7	57.5
20%	MR	39	40.4	40.6	56.5	57.4
20%	LR	38.4	41.4	42.2	56.7	56.9
5%	GR	39.1	41.5	41.8	55.6	56.5
5%	MR	39.9	40.2	39.3	56.2	55.4
5%	LR	38.7	39.0	37.9	52.2	53.6

was calculated using Equation 1, assuming that flow discharge, Q, was proportional to contributing area, $Q \propto A$. The experiment was design to provide uniformity in soil properties and rainfall intensity. The large runoff rate (see Table 2) reduces quickly the possible spatial differences in surface storage due to the fast filling and breaching of closed depressions. Since spatial variability and storage have been largely eliminated in our experimental design, and since these two factors are what cause at bankfull discharge in river basins that $Q \propto A^a$ with $a < 1$ [*Leopold et al.*, 1964], we consider it justified to assume $Q \propto A$. In that case, equation 1 becomes:

$$E = \sum_{i=1}^{i=n} P_i = \sum_{i=1}^{i=n} k' L_i \sqrt{A_i} \qquad (4)$$

where k' is a constant that had the same value for all the links in the same network at a given flow discharge, A_i [L^2] is the contributing area for link i, and L_i [L] is the length of link i. The same value for k' was used for all six drainage networks for each set of runs (i.e., prior to initial rainfall and after each of the 5 rain periods). The implications of the assumption of a constant k' will be discussed. All of our analyses were made for the whole set of rills developed on the same flume surface, instead of disaggregating the surface into watersheds (or their equivalent in our context) formed by the links draining through a single outlet as is been usually done. This kind of aggregate analysis has been made previously in some drainage and rill experiments at plot and flume scale with multiple outlets [*Helming et al.*, 1998; *Lewis et al.*, 1994].

3. Results

[24] Figure 2 shows an example of the initial and final surface of each treatment at 20% slope, and also an example of the final surface of each treatment at 5% slope. They were obtained from the DEMs acquired with the laser scanner. The treatments at 20% slope developed an intensively rilled surface, with the number of rills decreasing with increasing surface roughness. The treatments at the 5% slope showed a lesser degree of rilling. They developed fewer rills, and those rills were wider and shallower than those at 20% slope. Table 3 quantifies those observations, each value being an average of the two replications per treatment. It can be seen in Figure 2 that for both slopes there was an intense destruction of the initial surface features, such as clods and tillage marks, as a consequence of rainfall impact and sheet flow. Soil consolidation was visually evident, especially for the MR and GR treatments. This consolidation is reflected in the bulk density of the top 0.05-m soil of the final surfaces which had a value of 1250 kg m^{-3}. No significant differences among the treatments for this final bulk density were detected, although only two replications were made per treatment. This value of bulk density was higher than those of the initial surfaces (Table 1).

[25] The general pattern was of a decrease of the soil surface level over the entire soil surface for all the treatments, except for GR at 5% slope. This general decrease was due to the combined action of erosion and consolidation. For GR at 5% slope the pattern was spatially more complex, with areas of net deposition combined with others of net erosion plus consolidation. The areas of net deposition corresponded, approximately, to depressions created during tillage. Figure 3 shows two profiles of the soil surface (in the direction perpendicular to the main slope) that illustrate these observations. The final runoff rates corresponding to the same rainfall intensity for each

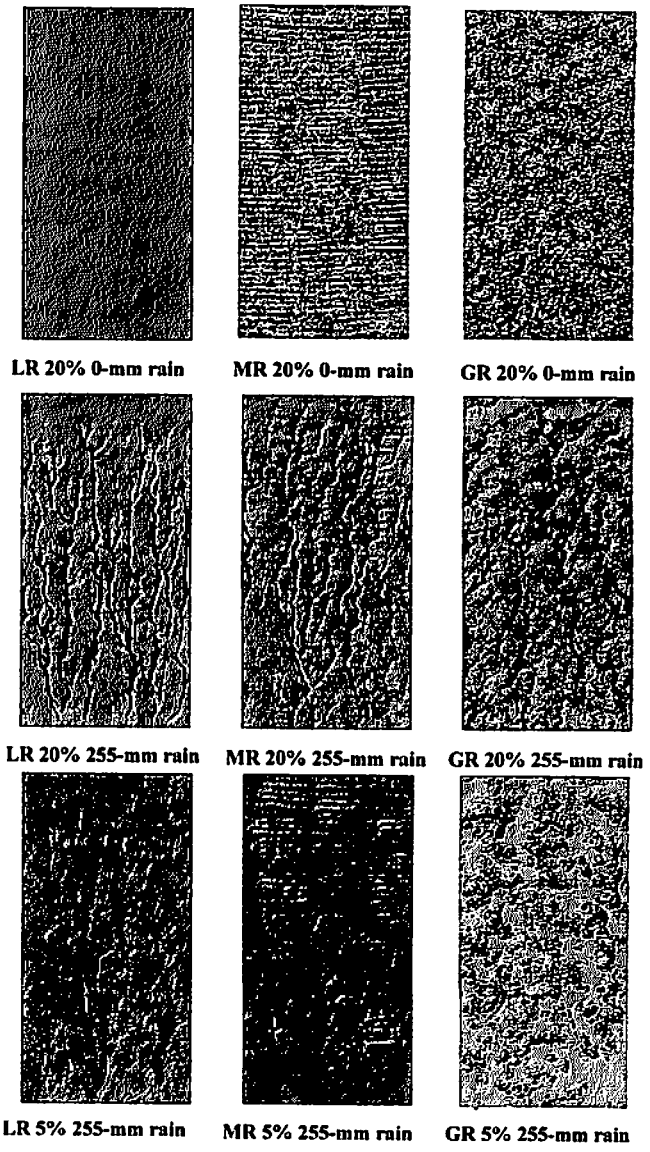

Figure 2. Examples of the digital elevation models of the initial and final surfaces, after 255 mm of rain.

Table 3. Average Rill Characteristics

Slope	Treatment	Average Number of Rills Per Transect	Average Rill Depth, mm	Average Rill Width, mm
20%	GR	7.5	32.6	36.1
20%	MR	10.5	36.2	26.8
20%	LR	10.6	44.3	41.8
5%	GR	4.1	4.4	70.6
5%	MR	4.8	5.0	57.7
5%	LR	5.8	6.1	53.0

treatment were similar, while the final runoff rates for the treatments at 20% slope were slightly greater than those corresponding to 5% slope (Table 2).

[26] Figure 4 gives an idea of the performance of the routing algorithms in reproducing the observed rill network. At 20% slope the delineated network showed a close resemblance with the observed one, with no apparent differences due to the routing method. At 5% slope the delineated network still occupied the areas of incision by flowing water, but the match seems to be less precise than that at 20% slope. At 5% slope there were some minor differences between the networks delineated using a multiflow method and the networks determined using the D8 method. Despite that, both methods agree in the general structure of the delineated networks at 5% slope. Table 4 shows the values (average of two replications) for the CSA, reflecting an increasing threshold area for lesser slope, and an apparent trend toward larger CSA for smoother surfaces. Although for consistency with other published analysis we used a time-constant CSA value in our analysis, it is interesting to note that the CSA calculated after each rainfall varied little at the 20% slope (1% reduction from the CSA after the first simulation to that after the fifth one, average of all treat-

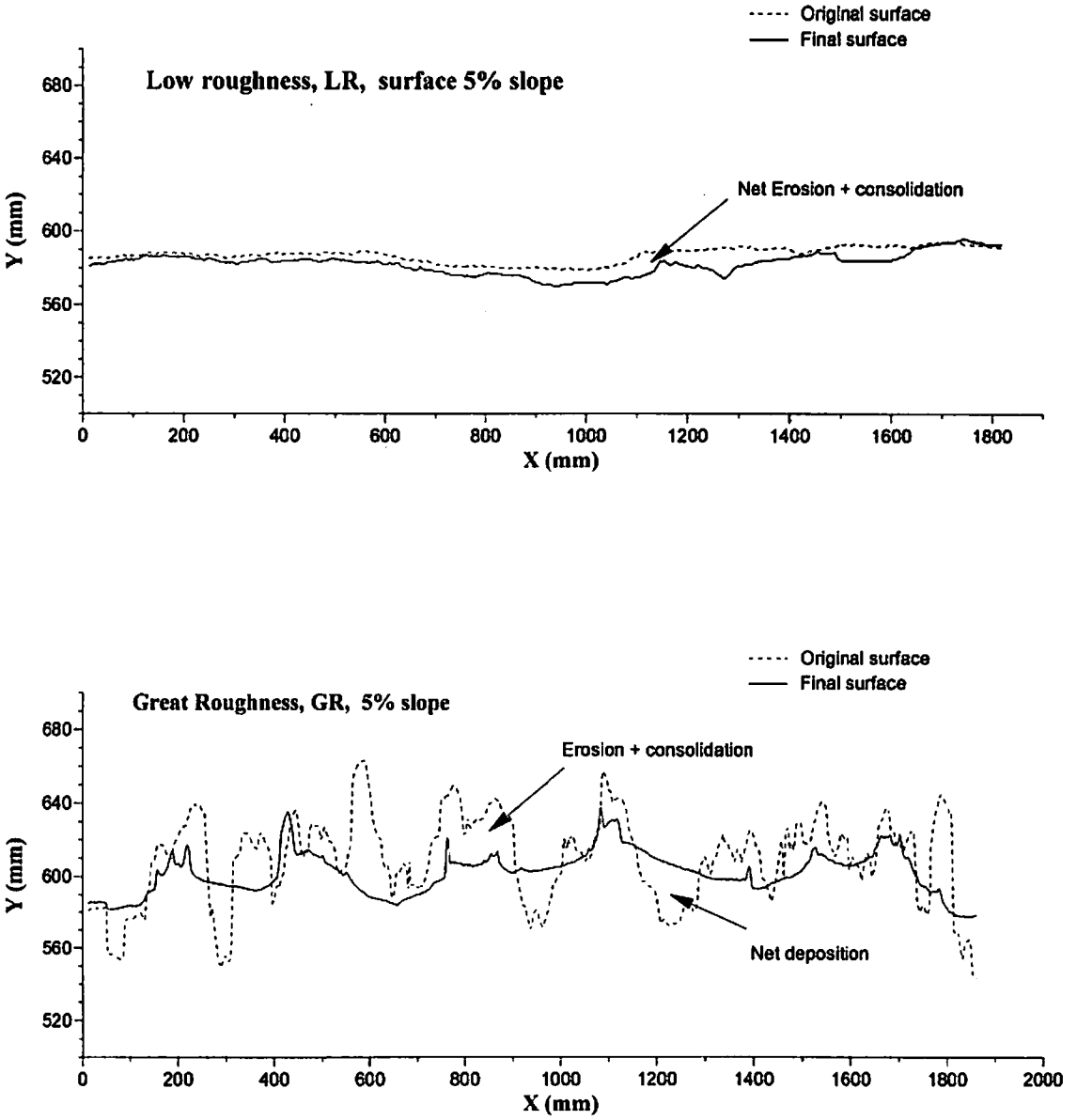

Figure 3. Examples of profiles of the initial and final soil surface, in the direction perpendicular to the main slope.

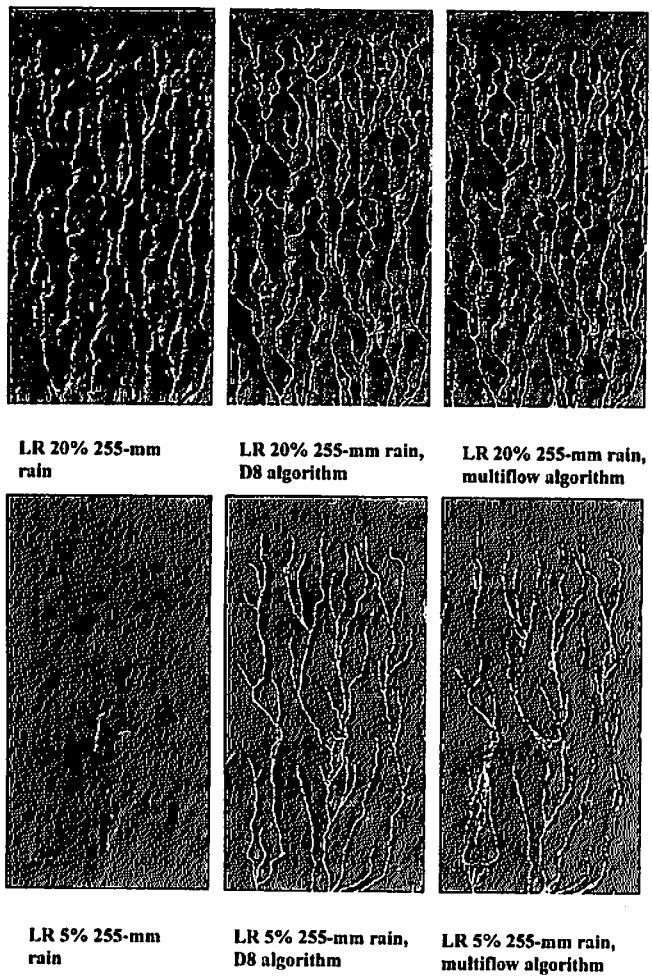

Figure 4. Comparison of the delineated networks obtained using a single flow, D8, or a multiflow algorithm to calculate flow accumulation.

ments), while it did vary significantly at the 5% slope (66% reduction from the CSA after the first simulation to that after the fifth one, average of all treatments). This is a consequence of the fact that at 20% the rill networks developed quickly and spread throughout the flume surface within the first rainfall simulation, following the model reported by *Parker* [1977] for a flume with a stable base level. At the 5% slope, due to smaller erosive power of the overland flow (Table 2), much more surface runoff flowing through the drainage network was required to incise the flume surface.

[27] Figures 5 to 7 show examples of the evolution of the networks for all the treatments. The networks exhibited a clear transformation through the successive rainfalls. Some features of the original drainage networks were still recognizable in the final surface of the GR 5% slope, suggesting that the effect of the initial microrelief still dominated the network structure after 255-mm of rainfall. Figures 8 to 11 (showing averages of the two replications) show the evolution of some of the network links characteristics. The average link slope (Figure 8) increased with cumulative rainfall for all the treatments, except for GR 5%, evolving toward a value approximately the same as that of the main slope. These values reached a plateau for the 5% slope treatments (including GR, where it decreased slightly before leveling off). At the 20% slope the evolution appeared to be continuing through the entire experiment, although at a decreasing rate.

[28] The average link sinuosity (Figure 9) tended toward a narrow range of values for all the treatments, with most of the variation occurring in the first 135-mm of rainfall. The average link sinuosity increased slightly during the experiment for the LR surface at 20% slope, while all the other treatments showed decreases in their sinuosity. The average link network orientation (Figure 10) also evolved during the experiment, with a decrease (that is, orienting toward the direction of the main slope) for MR and GR surface, but a slight increase for the LR surface at 20%. Drainage density (Figure 11) evolved in all the treatments, slightly in MR and GR and more clearly in LR. It decreased in all the treatments except in GR at 5% slope.

Table 4. Contributing Threshold Area in Number of Cells, CSA, Used for the Determination of the Networks, for Each Slope and Treatment

Treatment	20% Slope	5% Slope
GR	1675	3950
MR	1600	3800
LR	1759	4400

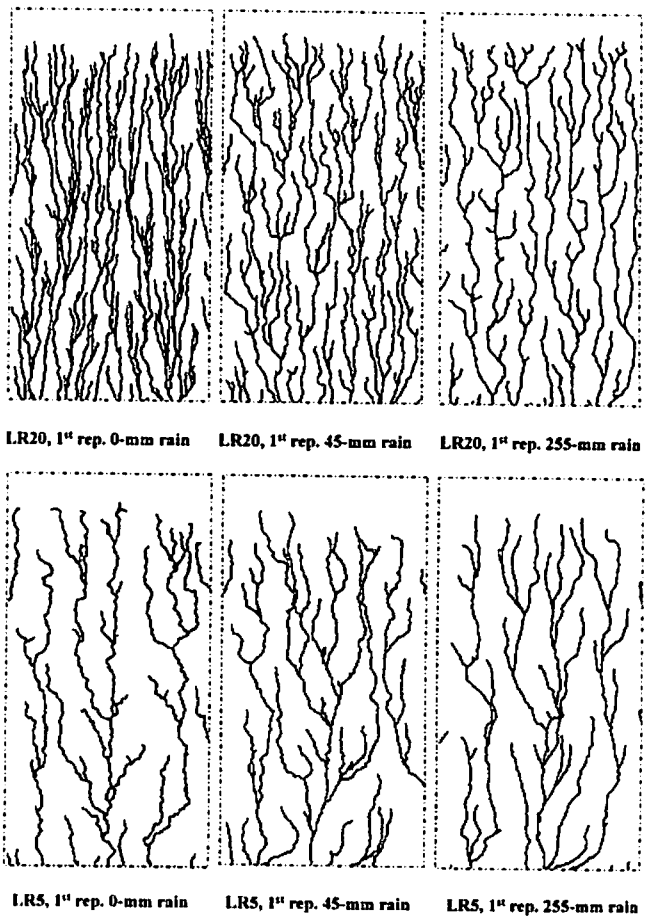

Figure 5. Example of the networks evolution for the LR treatment.

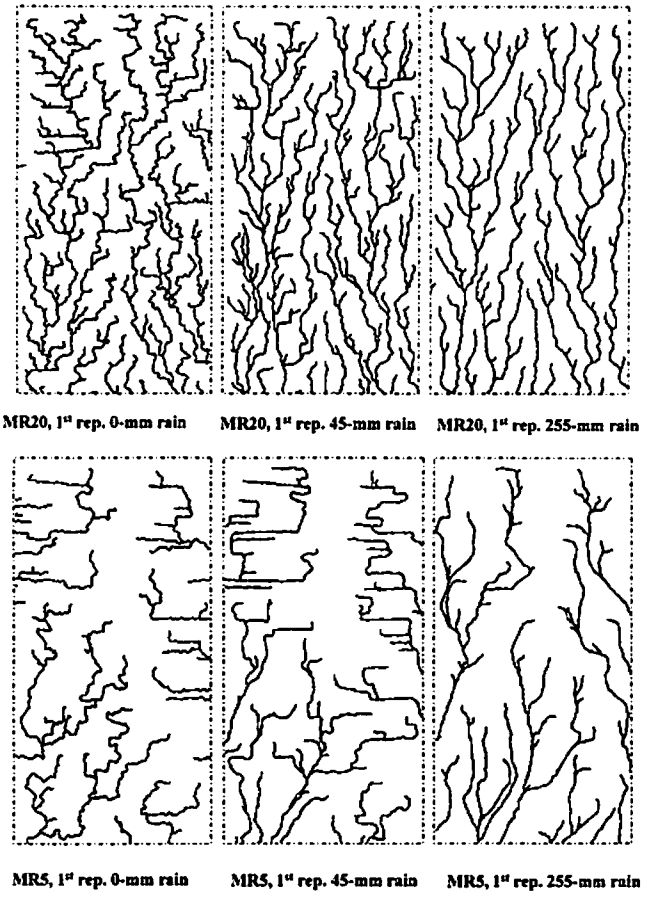

Figure 6. Example of the networks evolution for the MR treatment.

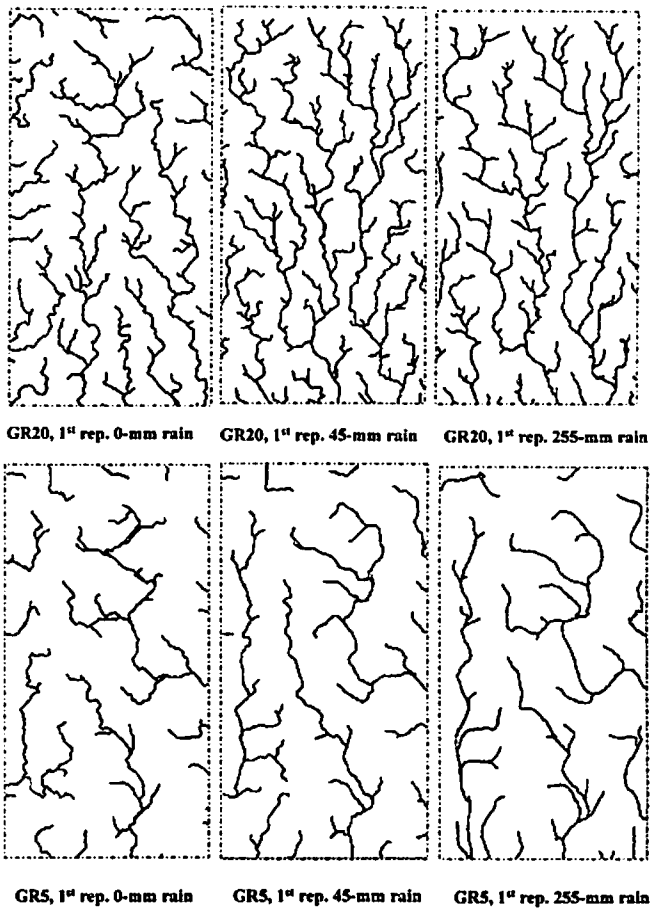

Figure 7. Example of the networks evolution for the GR treatment.

[29] The evolution of rate of energy expenditure of all the links within the flume surface according to equation 4 is shown in Figure 12. To facilitate the comparison, all the values corresponding to the 6 DEMs belonging to the same session of rainfall simulations were normalized dividing by the E_i corresponding to the initial surface for that session at zero rainfall, E_o. All the treatments at 20% slope showed a sustained decrease of E_i:E_o with cumulative rainfall. This was observed also in the LR surface at 5% slope. The MR surface with 5% slope showed a decrease in E_i:E_o with respect to the surface after the first 45-mm of rainfall, but it never decreased to values smaller than those corresponding to the original undisturbed surface. The GR surface at 5% slope showed a general increase in E_i:E_o during all the rainfall simulation, although the rate seems to decrease around 200-mm rainfall.

[30] Figure 13a was constructed from the flow velocities made in selected rills during the fifth rainfall simulation of each treatment, and the flow discharge at each of those rills estimated from the cumulative area of the same rill links calculated from the DEM's multiplied by the runoff coefficient determined from the plot final runoff rate. They provide an idea of the variation of flow velocity within the rills at a given flume discharge showing a large scatter but no clear relationship with flow discharge. Flow velocity at a given link usually increased with rainfall intensity (Figure 13b). The other treatments not shown in Figure 13 showed similar trends.

[31] Figures 14a and 14b show examples of the relationship between link slope, S_i, and link contributing area, A_i, obtained for the 20% and 5% slope treatments, respectively, according to $S_i = a A_i^{\alpha}$. Each point in Figure 14 corresponds to the average of 10 values. For the 20% slope treatments the general trend was that observed in Figure 14a: a trend

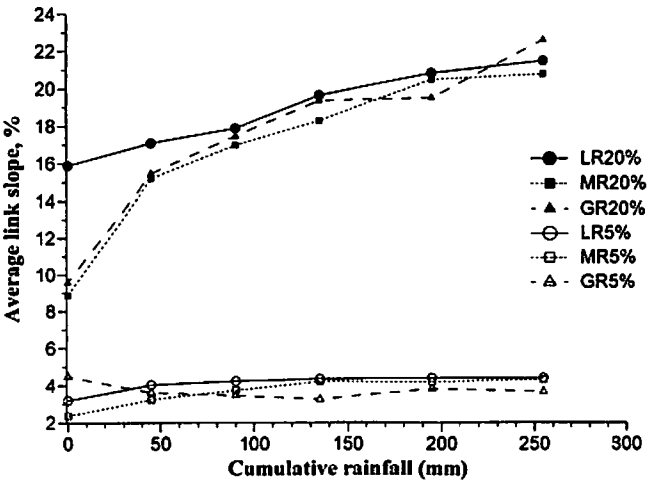

Figure 8. Evolution of the average link slope with cumulative rainfall.

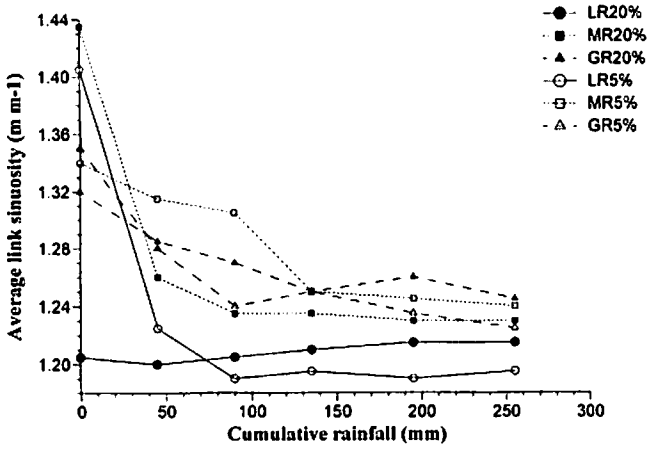

Figure 9. Evolution of the average link sinuosity with cumulative rainfall.

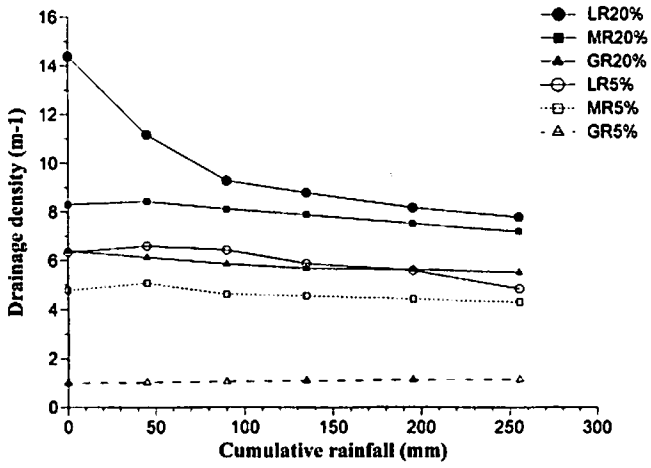

Figure 11. Evolution of the drainage density with cumulative rainfall.

from no clear relationship on the original surface toward an inverse relationship between slope and contributing area, although with some scatter, after 255-mm rainfall. At 5% slope (Figure 14b) we did not observe any relationship between slope and contributing area, with low r^2 and α values close to zero.

4. Discussion

[32] Rill networks developed from the same average slope with different initial surfaces showed different average link properties, such as average number of rills, drainage density, and mean link orientation. This was especially clear when comparing the low and moderate roughness treatments (LR and MR) with the great roughness (GR) treatment. Differences between MR and LR were less clear. This result suggested that although the network characteristics evolved sometimes in a converging way, such as for the case of the mean link slope, the effect of the initial microrelief persisted after a substantial amount of rainfall, e.g. for the case of mean link orientation. One could question whether the initial surfaces considered in our experimental design were too artificial and produced results not representative of tilled areas. The values of roughness on the LR and MR treatments were slightly smaller to those observed in the field, and GR represented a large un-oriented roughness that can be found in mechanized arable land, and in hand-tilled areas. We should expect often to see in field situations an oriented roughness, which suggests that the differences due to the surface roughness should be comparable to those observed in our flume. Empirical models of flow convergence at the field scale implicitly recognize this. These models consider soil roughness [*Souchere et al.*, 1998], or soil roughness and tillage aspect [*Takken et al.*, 2001] to be dominant factors below a threshold value of slope steepness, but curiously, contributing area had a small effect on the direction of flow [*Takken et al.*, 2001]. The effect of large roughness on flow direction has to be addressed in future studies to allow correspondence between results of laboratory and field experiments, and between empirical and physically based approaches.

[33] Previous studies have shown concern about the effect of the routing method on the delineated network. Our results showed that for situations where rilling is predominant and a high resolution DEM is available, this does not constitute a major concern, and the D8 algorithm

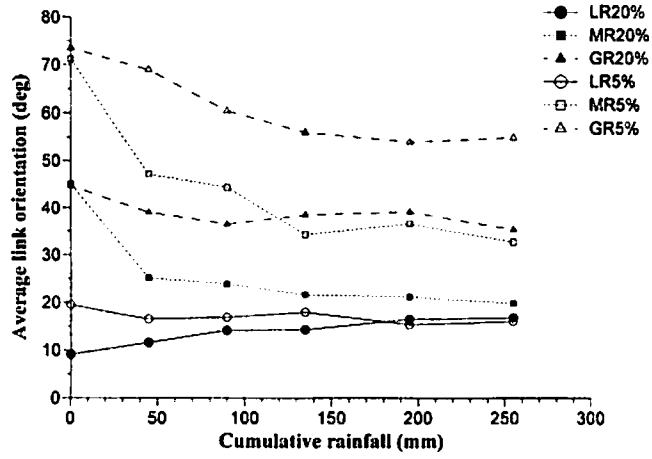

Figure 10. Evolution of the average link orientation with cumulative rainfall.

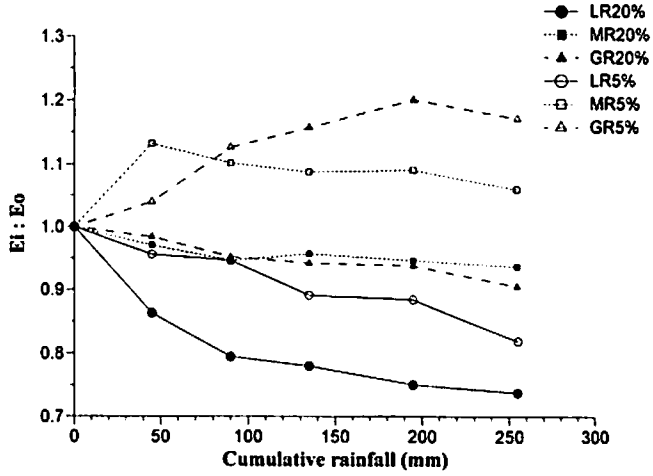

Figure 12. Evolution of E, described by equation 4, during the network development under successive rainfalls.

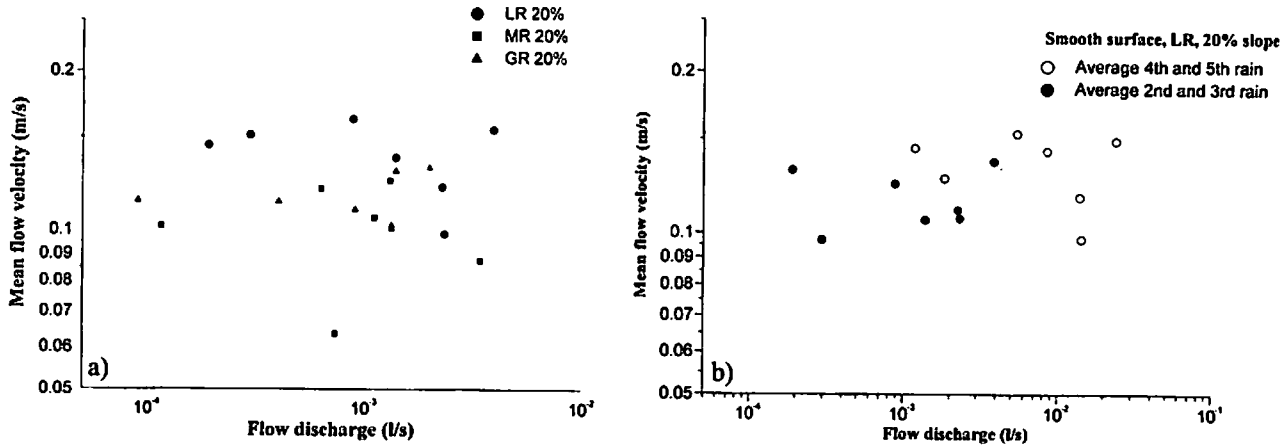

Figure 13. Flow velocity versus flow discharge at selected rills for during the fifth rainfall simulation corresponding to one replication of each treatment at 20% slope (a) and flow velocity at different rainfall intensities corresponding to the same LR 20% replication (b).

provides a reasonable description of the observe rill network. That was the case of the treatments at 20% slope, where also the use of a time-constant CSA value was reasonable due to the quick development of the rills. The results obtained for the 5% slope treatments, where rilling was not intense (see Figure 4 at 5% slope and compare the networks on the lower left side of the DEMs), suggest that there is a limit for the reliability of the D8 method in depicting the actual drainage network. With nonappreciable zones of flow incision on the surface, a multiflow algorithm, like the Quinn method, predicts several lines of accumulation flowing more or less parallel to each other, like in some areas of Figure 4. This represents areas where a sheet of water flows on a relatively wide area, something that we observed in the flume in the 5% slope treatments. This area of localized wide shallow flow contrasts with the impression of concentrated flow suggested by the single link predicted by the D8 method for the same zone. The D8 method has become something of a standard in network studies, and it is likely to maintain that status in the near future. Our relatively large CSA, compared to that from other drainage network studies at this scale, suggest that we are near to the conditions where the D8 algorithm starts introducing artificial flow concentration in the analysis. For this reason some kind of validation of the delineated network, even if it is only by visual comparison with the observed rill or flowing areas, should always be made, and improved methods of delineating flow networks deserve more attention in further studies at small-scale drainage and rill network studies. Additionally, due to the slow emergence of the rilled areas at the 5% slope treatments, the assumption of a time-constant CSA value may have been problematic since the treatment depicted a network where, at the initial stages, rilled and nonrilled areas coexisted. Despite this being a general assumption, even assumed by us for consistency with other published works [e.g., *Helming et al.*, 1998], improved analysis addressing these issues and separation between rilled and nonrilled areas in future small-scale network studies is needed.

[34] The networks evolved through successive rainfall simulations following certain patterns. Drainage density tended to decrease, although the magnitude of this decrease

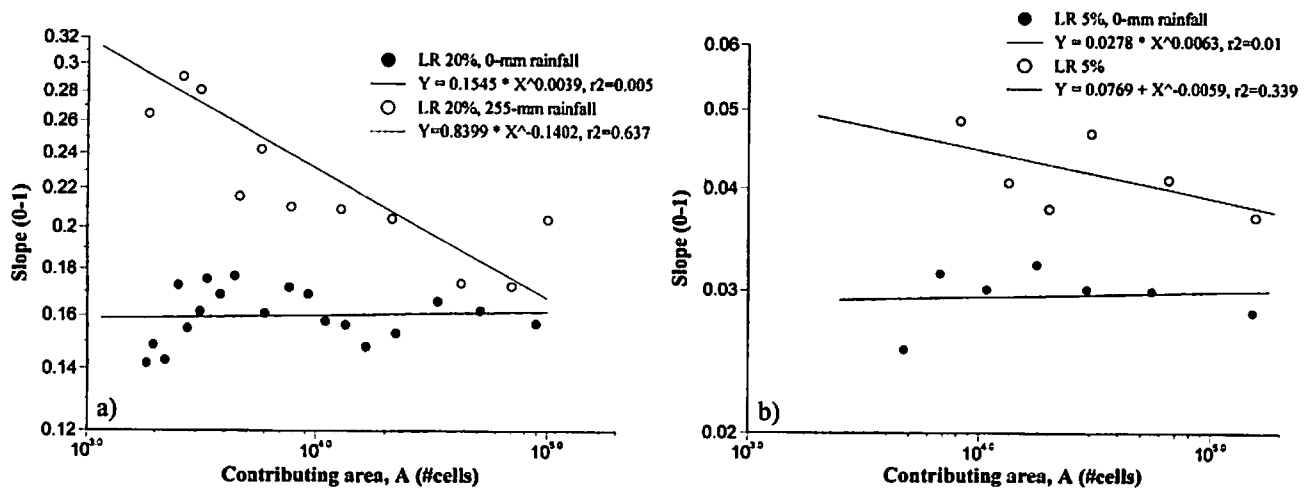

Figure 14. Examples of the link slope-area relationship, $S_i = a A_i^{\alpha}$, for the initial and final surfaces at 5% (a) and 20% slope (b).

was large only for the LR treatments. Mean link sinuosity decreased for all the treatments, with the exception of a very mild increase LR at 20% slope. We attribute this mild increase to the development of some cracks on the surface between rainfalls that affects what are very straight links compared to the other treatments. The average link sinuosity trend toward similar values after 255-mm rain for all the treatments. Mean link slope also took similar final values for the different treatments at the same slope. This similarity in final average link values suggests that the mechanisms controlling the evolution at link scale were not affected by the initial microrelief, while microrelief had a significant effect on the general structure of the network, reflected in properties such as mean link orientation and drainage density that did not converge for different treatments.

[35] During the evolution of all the treatments at 20% slope and LR at 5% slope the sum of the square root of the contributing area times the length of each link was minimized. This may have important implications for future modeling studies since the data provide a magnitude that can be used as the key variable in the evolution of drainage networks in steep or moderate slopes with smooth surface. The effect of large roughness and moderate slopes needs additional study. It is important to note that it requires only topographical information, which simplifies the inputs required by models. These kind of studies are not new at basin scales, and what we envision here for rill networks are analyses in the line of that made by *Rinaldo et al.* [1992] or *Sun et al.* [1994] employing optimal channel networks, OCN, or approximate models as the slope-area model used by *Ijjáz-Vásquez et al.* [1993]. They may provide insight into the evolution of rill networks at hillslope scales. To do this analysis, progress into algorithms, or in approximate solutions, with the ability to cope with DEMs formed by millions of cells will be required.

[36] The translation of the magnitude described by equation 4 into a rate of energy dissipation relies on the validity of the assumption of optimality at each link, something that still needs to be proven for small-scale rill networks, although our discussion assumes that assumption to be valid. All the surfaces at 20% slope, and LR at 5% slope showed reduction of the global rate of energy dissipation according to equation 4, while for MR and GR they did not. The relative decrease observed in the treatments was not large (between 5 and 25%), but it is within the range observed by *Rinaldo et al.* [1992] in OCN simulations.

[37] We attribute the differences in the evolution of E according to equation 4 between the treatments at 20 and 5% to the differences in the processes dominating water erosion at both slopes. At 20% slope, erosion by concentrated flow (rilling) is the dominant process, while at 5% diffusive processes as rain splash, soil clod redistribution by gravity and sheet flow seem to be important factors in controlling the erosion process. This seems apparent from comparison of the final surfaces, see Figure 2. Additionally, the trend toward a relationship with a negative exponent (ranging from -0.20 to -0.15) between link slope and contributing area at 20% slope (Figure 14a) seems to support the dominance of concentrated flow processes. This is based on analyses of river basins by *Willgoose et al.* [1991a], who consider the link slope-contributing area relationship as the signature of the dominance of fluvial transport processes over diffusive ones. The inversion of the sign in the exponent of that relationship would indicate, according to the same authors, the dominance of diffusive transport processes. The lack of correlation between slope and contributing area in Figure 14b, can be interpreted as a transition between rilling and diffusion as dominant processes. We considered an acceptable fit as approximately $r^2 = 0.6$ (as that shown in Figure 14b). This correlation level is not far from some relationships shown for mature river networks in which large scatter has also been observed [*Willgoose et al.*, 1991a].

[38] *Tarboton et al.* [1992] has shown that the relationship between slope and contributing area can be difficult to detect when a relatively small amount of noise is present in the elevation data from DEMs. Some degree of error is present in any dataset due not only to measurement errors, which we showed to be relatively small in our study, but also because of the modifications in elevations from filling or breaching closed depressions that take place prior to the calculation of the drainage network from the DEMs. The effect of this noise would be more important at 5% slope, where the average link slope was smaller. Despite this, we still interpret the results for MR and GR as a result of the lack of dominance of rilling based on observations (Figures 2 and 3), the values obtained for the dimensionless index described by equation 5 (commented a few lines later), and the low correlation between slope and contributing area (r^2 values around 0.1, graphs not shown).

[39] We do not have, however, a clear interpretation of the apparent contradiction for LR at 5% between Figure 12, where it evolved similarly to the surfaces with intensive rilling (i.e., the 20% slopes), and Figure 14b where it did not show a clear relationship between link slope and contributing area. It is possible that we are in a situation where the noise in the elevation data and the small number of links make it impossible to detect a relationship that might exist.

[40] To further clarify this point, we used the index proposed by *Willgoose et al.* [1991b], equation 5, to compare the relative importance between fluvial and diffusive transport between two catchments:

$$ID = \frac{DED_{(1)}}{DED_{(2)}} \tag{5}$$

where ID is calculated according to *Willgoose et al.* [1991b], and the subscripts refer to different catchments. The DED terms represent a combination of many different variables described in detail by *Willgoose et al.* [1991b]. In our case the subscript (1) refers to surfaces at 20% slope, and the subscript (2) refers to those at 5% slope. An ID value equal to 1 means that the relative importance of fluvial (concentrated flow) and diffusive transport is the same in both catchments. An ID value lower than one indicates that diffusive processes are less dominant in catchment 1. In our case the ID value calculated for the average conditions of catchments 1 and 2 (20 and 5%) was 0.11, indicating a much larger importance of diffusive processes at the 5% slope. It would be interesting to study the evolution of networks at 5% slope under more intense rainfall or longer rainfall simulation to see if there is a point at which there is a transition toward rill dominated erosion process.

[41] The assumption of similar flow velocities within the network links seems a reasonable approximation according

to our results (Figure 13), due to the lack of correlation of velocity with flow discharge. Attention needs to be given in further studies to the large scatter showed in Figure 13, to distinguish if that is only an artifact of the experimental technique used to measure flow velocity or if the variability is real. Published data of mean flow velocity versus flow discharge in rills [e.g., *Govers*, 1996, Figure 9] show also a large scatter, meaning that for a small interval of flow discharge (as occurs in our experiment) no correlation between both variables seems to exist. This suggests that our experimental data may not be an artifact, although more rigorous testing using more precise techniques is needed.

[42] The subset formed by the 3 surfaces corresponding to the three rainfalls at 45 mm h^{-1} intensity fulfill the conditions of similar runoff rate and mean flow velocity that supports the use of a constant k value for the surfaces after the simulations. This indicates that the global rate of energy expenditure is minimized through the network evolution, always assuming the validity of a local optimality principle. We think that this subset shows a correspondence in network evolution processes at two very different spatial and temporal scales, rills and rivers. We state this because the data show the optimization of the global rate of energy dissipation according to *Rodríguez- Iturbe et al.* [1992], equation 4; and also they follow, with $Q \propto A$, the global optimization principle outlined by *Sun et al.* [1994] with the use of the average value of 0.5 proposed by them for α in equation 6, where all the other variables have been previously defined.

$$E = \sum_{i=1}^{i=n} P_i = \sum_{i=1}^{i=n} Q_i^{\alpha} L_i \qquad (6)$$

This is a step forward, experimentally, from the previous studies based on the comparison of the topological or fractal properties [e.g., *Wilson and Storm*, 1993] of rill networks.

[43] These results also suggest that the theory developed for river networks might explain the evolution of rill networks at the hillslope scale under similar situations of intensive rilling created in our experiment. The interpretation of the whole dataset, including the initial undisturbed surface and those after 60 mm h^{-1} rainfall, is more complicated since we cannot maintain the assumption of a constant k' due to the increase in mean flow velocity and flow discharge. In our experiment the increases in runoff and flow velocity induced by the increases in rainfall intensities are relatively small, and we can assume that they do not alter significantly the patterns of overland flow circulation. This is especially true considering that, due to the intensive rilling, when the fourth rainfall simulation starts the rills are deep enough to accommodate that additional discharge without overflowing. In this situation it seems reasonable to analyze the whole data set for a theoretical maximum discharge constant for all the situations. This is something similar to the consideration made by *Rodríguez-Iturbe et al.* [1992], assuming that their analysis corresponds to a mean discharge of constant value that controls the evolution of the river network. Nevertheless, we think that the theoretical interpretation of the minimization of the magnitude defined by equations 4 and 6 deserves further analysis and experimental studies under different rainfall intensities.

[44] As presented in the introduction, river networks evolve according to a global and a local principle of energy expenditure. The only approximation of our analysis to the local principle has been the suggestion that a trend toward a constant mean flow velocity may hold for rill networks at hillslopes, which is a consequence of the local optimality assumption according to *Rodríguez-Iturbe et al.* [1992]. More precise studies about the flow velocity variation within the network may provide insight into the similarity between both scales on this local optima principle. Studies of the downstream hydraulic relationships of the rills for a given flow discharge may also provide insight about similarity between both scales, an analysis that we expect to make in the near future using the same dataset presented in this paper.

5. Summary and Conclusions

[45] Our results showed an experimental confirmation, assuming the validity of a local optimality principle, that rill networks evolved according to the global rate of energy dissipation of network links presented on the flume surface for the situations where intensive rilling (i.e., at 20% slope) occurred. At 5% slope, where diffusive transport played a major role in the erosion process, we did not observe the same process of evolution for the medium roughness and large roughness surfaces, while the results for the low roughness surface at the 5% slope remain inconclusive. This similarity suggest that simulation of rill networks by optimizing the global rate of energy expenditure, or simplified models such as the slope area model, may be experimentally justified. This result may provide alternative methods to modeling rill network initiation and evolution. Further research is needed to interpretate the evolution of equations 4 and 6 under different rainfall conditions, and to study the spatial distribution of flow velocity within the networks for a given flow discharge.

[46] Additional research needs to be done on rill and drainage network delineations at moderate slopes and rough surfaces where rilling and flow concentration is less active. Also, more work is needed on the evolution of drainage and rill networks in situations of small rilling intensity, as those in the 5% slope treatments presented here, where we did not observed correspondence with fluvial processes. Other possible steps in the study of the similarity between fluvial and rill scales may be the analysis of the local rate of energy expenditure at the rill link scale and the study of the downstream hydraulic relationships at a given flow discharge.

[47] **Acknowledgments.** We acknowledge Chi-hua Huang from the National Soil Erosion Research Laboratory at West Lafayette, IN, for the use of his last generation of laser scanner during the extended period of time required by our experiment, as well as for his advice. We also acknowledge Michael Woldenberg from the State University of New York at Buffalo for his comments and suggestions about the interpretation of our experimental results and the comments made by two anonymous reviewers that helped improve the quality of the manuscript. Most of the experiment took place while the first author was supported by a grant from the Spanish Ministry of Science and Technology, support that is gratefully acknowledged.

References

Banavar, J. R., F. Colaiori, A. Flammini, A. Maritan, and A. Rinaldo, Scalin, otimality, and landscape evolution, *J. Stat. Phys.*, *104*(1/2), 1–48, 2001.

Blake, G. R., and K. H. Hartge, Bulk density, in *Methods of Soil Analysis*, part I, *Physical and Mineralogical Methods*, edited by A. Klute, *Agron. Monogr.*, vol. 9, 2nd ed., pp. 363–375, Am. Soc. of Agron., St Joseph, Mich., 1986.

Boiffin, J., La degradation structurale des couches superficielles sous l'action des pluies, thése de docteur-ingéneur, Inst. Natl. Agron., Paris, 1984.

Currence, H. D., and W. G. Lovely, The analysis of soil surface roughness, *Trans. ASAE*, *13*(6), 710–714, 1970.

Darboux, F., and C. Huang, An instantaneous-profile laser scanner to measure soil survey micro-topography, *Soil Sci. Soc. Am. J.*, *67*, 92–97, 2003.

Favis-Mortlock, D. T., J. Boardman, A. J. Parsons, and B. Lascelles, Emergence and erosion: A model for rill initiation and development, *Hydrol. Processes*, *14*, 2173–2205, 2000.

Flanagan, D. C., and M. A. Nearing, USDA-water erosion prediction project: Hillslope profile and watershed model documentation, *NSERL Rep.2*, Agric. Res. Serv., West Lafayette, Indiana, 1995.

Garbrecht, J., and L. W. Martz, TOPAZ: An automated digital landscape analysis tool for topographic evaluation, drainage identification, watershed segmentation and subcatchment parameterization, TOPAZ user manual, *ARS Publ. GRL 97-4U.S.*, Grazinglands Res. Lab., Agric. Res. Serv., El Reno, Okla., 1997.

Govers, G., Soil erosion process research: A state of the art, *Klasse de Wetenschappen, Jaargang 58*, Paleis der Academiën, Brussells, 1996.

Gyasi-Agyei, Y., G. Willgoose, and F. D. De Troch, Effects of vertical resolution and map scale of digital elevation models on geomorphological parameters used in hydrology, *Hydrol. Processes*, *9*, 363–382, 1995.

Helming, K., M. J. M. Römkens, S. N. Prasad, and H. Sommer, Erosional development of small scale drainage networks, in *Process Modelling and Landform Evolution*, edited by S. Hergarten and H. Neugebauer, pp. 123–146, Springer-Verlag, New York, 1998.

Horton, R. E., Erosional development of streams and their drainage basins; hydrophysical approach to quantitative morphology, *Geol. Soc. Am. Bull.*, *56*, 275–370, 1945.

Howard, A. D., Optimal angles of stream junction: Geometric, stability capture, and minimum power criteria, *Water Resour. Res.*, *7*(1), 863–873, 1971.

Howard, A. D., Theoretical model of optimal drainage networks, *Water Resour. Res.*, *26*(9), 2107–2117, 1990.

Ijjáz-Vásquez, E., R. L. Bras, I. Rodríguez-Iturbe, R. Rigon, and A. Rinaldo, Are river basins optimal channel Networks?, *Adv. Water Resour.*, *16*, 69–79, 1993.

King, W. H., and L. D. Norton, Methods of rill flow velocity dynamics, *Pap. 92-2542*, Am. Soc. of Agric. Eng., St. Joseph, Mich., 1992.

Knighton, D., *Fluvial Forms and Processes: A New Perspective*, Edward Arnold, London, 1998.

Leopold, L. B., M. G. Wolman, and J. P. Miller, *Fluvial Processes in Geomorphology*, W. H. Freeman, New York, 1964.

Lewis, S. M., B. J. Barfield, D. E. Storm, and L. E. Ormsbee, Proril—An erosion model using probability distributions for rill flow and desinty I. Model development, *Trans. ASAE*, *37*(1), 115–123, 1994.

Morgan, R. P. C., J. N. Quinton, R. E. Smith, G. Govers, J. W. A. Poesen, K. Auerswald, G. Chisci, D. Torri, and M. E. Styczen, The European soil erosion model (EUROSEM): A dynamic approach for predicting sediment transport from fields and small catchments, *Earth Surf. Processes Landforms*, *23*, 527–544, 1998.

Mosley, M. P., Experimental study of rill erosion, *Trans. ASAE*, *17*(5), 909–916, 1974.

O'Callaghan, J. F., and D. M. Mark, The extraction of drainage networks from digital elevation data, *Comput. Vision Graphics Image Proc.*, *28*, 323–344, 1984.

Ogunlela, A., B. N. Wilson, C. T. Rice, and G. Couger, Rill network development and analysis under simulated rainfall, *Pap. 89-2112*, Am. Soc. of Agric. Eng., St. Joseph, Mich., 1989.

Parker, R. S., Experimental study of drainage system evolution and its hydrologic implications, Ph.D. dissertation, Colo. State Univ., Fort Collins, 1977.

Quinn, P. F., K. J. Beven, P. Chevalier, and O. Planchon, The prediction of hillslope flow paths for distributed hydrological modeling using digital terrain models, *Hydrol. Processess*, *5*, 59–79, 1991.

Rieke-Zapp, D., H. Wegman, F. Santel, and M. Nearing, Digital photogrammetry for measuring soil surface roughness, paper presented at the Annual Meeting, Am. Soc. of Photogrametry and Remote Sens., St. Louis, Mo., 23–27 April 2001.

Rinaldo, A., I. Rodríguez-Iturbe, R. Rigon, R. L. Bras, E. Ijjász-Vasquez, and A. Marani, Minimum energy and fractal structures of drainage networks, *Water Resour. Res.*, *28*(9), 2183–2195, 1992.

Rodríguez-Iturbe, I., and A. Rinaldo, *Fractal River Basins: Chance and Self-Organization*, Cambridge Univ. Press, New York, 1997.

Rodríguez-Iturbe, I., A. Rinaldo, R. Rigon, R. L. Bras, A. Marani, and E. Ijjáz-Vásquez, Energy dissipation, runoff production, and the three-dimensional structure of river basins, *Water Resour. Res.*, *28*(4), 1095–1103, 1992.

Roy, A. G., Optimal models of river branching angles, in *Models in Geomophology*, edited by M. J. Woldenberg, pp. 269–285, Allen and Unwin, Concord, Mass., 1985.

Shreve, R. L., Statistical law of stream numbers, *J. Geol.*, *74*, 17–37, 1966.

Song, C. S. S., and C. T. Yang, Minimum stream power: Theory, *J. Hydraul. Div. Am. Soc. Civ. Eng.*, *106*(HY9), 1477–1487, 1980.

Souchere, V., D. King, J. Daroussin, F. Papy, and A. Capillon, Effects of tillage on runoff directions: Consequences on runoff contributing area with agricultural catchments, *J. Hydrol.*, *206*, 256–267, 1998.

Sun, T., P. Meakin, and T. Jøssang, The topography of optimal drainage basins, *Water Resour. Res.*, *30*(9), 2599–2619, 1994.

Takken, I., G. Govers, V. Jetten, J. Natchtergaele, A. Steegen, and J. Poesen, Effects of tillage on runoff and erosion pattern, *Soil Tillage Res.*, *61*, 55–60, 2001.

Tarboton, D. G., R. L. Bras, and I. Rodríguez-Iturbe, A physical basis for drainage density, *Geomorphology*, *5*, 59–76, 1992.

Tarr, R. S., and L. Martin, *College Physiography*, Macmillan, New York, 1914.

Walker, J. P., and G. R. Willgoose, On the effect of digital elevation model accuracy on hydrology and geomorphology, *Water Resour. Res.*, *35*(7), 2259–2268, 1999.

Willgoose, G., R. L. Bras, and I. Rodríguez-Iturbe, A physical explanation of an observed link area-slope relationship, *Water Resour. Res.*, *27*(7), 1697–1702, 1991a.

Willgoose, G., R. L. Bras, and I. Rodríguez-Iturbe, A coupled channel network growth and hillslope evolution model: 2. Nondimensionalization and applications, *Water Resour. Res.*, *27*(7), 1685–1696, 1991b.

Wilson, B. N., and D. E. Storm, Fractal analysis of surface drainage networks for small upland areas, *Trans. ASAE*, *36*(5), 1319–1326, 1993.

Yang, C. T., Potential energy and stream morphology, *Water Resour. Res.*, *7*(2), 311–323, 1971a.

Yang, C. T., On river meanders, *J. Hydrol.*, *13*, 231–253, 1971b.

Yang, C. T., C. S. S. Song, and M. J. Woldenberg, Hydraulic geometry and minimum rate of energy dissipation, *Water Resour. Res.*, *17*(4), 1014–1018, 1981.

Ziegler, T. R., and D. R. Wolf, Soil Survey of Tippecanoe County Indiana, Nat. Resour. Conserv. Serv., Washington, D. C., 1998.

F. Darboux, Laboratoire de science du sol, INRA, BP 20619, F-45166 Olivet Cedex, France. (Frederic.Darboux@orleans.inra.fr)

J. A. Gómez, Instituto de Agricultura Sostenible, CSIC, Apartado 4084, 14080 Cordoba, Spain. (ag2gocaj@uco.es)

M. A. Nearing, USDA-Agricultural Research Service, 2000 E. Allen Rd. Tucson, AZ 85719, USA. (mnearing@tucson.ars.ag.gov)